Available online at www.sciencedirect.com
SCIENCE DIRECT®
ELSEVIER
Journal of Magnetism and Magnetic Materials 293 (2005) 464–472
Journal of magnetism and magnetic materials
www.elsevier.com/locate/jmmm

Signal transduction by erythrocytes on specific binding of doxorubicin immobilized on nanodispersed magnetite

Olga Mykhaylyk[a,*], Anatoliy Kotzuruba[b], Nataliya Dudchenko[a], Gyula Török[c]

[a]*Institute Applied Problems Physics & Biophysics, NAS, Sluzhbova 3, UA-03142 Kyiv, Ukraine*
[b]*Institute of Biochemistry, NAS, Leontovicha 9, UA-01030 Kyiv, Ukraine*
[c]*Research Institute for Solid State Physics and Optics, H-1525 Budapest, P.O. Box 49, Hungary*

Available online 12 April 2005

Abstract

Two specific binding sites for doxorubicin were revealed at the plasma membrane of human erythrocytes on investigation of the binding of doxorubicin magnetic nanoconjugates. Free and conjugated doxorubicins modulated signal transduction in erythrocytes in a similar way. Both up-regulated nitric oxide and cyclic GMP (cGMP) and down-regulated cyclic AMP (cAMP) production and stabilize the membranes of damaged erythrocytes.

Keywords: Doxorubicin; Drug-conjugate; Erythrocytes; Plasma membrane; Signal transduction; SANS; Nitric oxides (NO); cAMP; cGMP; Hemolysis; Nanodispersed magnetite; Hydroxyethylstarch; O-(2-Aminoethyl)polyethylene glycol

1. Introduction

Doxorubicin (DOX), whose principle target was previously thought to be DNA, has been shown to exert its cytotoxic action solely by cell surface interaction since extracellular drug was required to initiate the cytotoxic cascade [1,2]. These findings initiated studies with DOX conjugates to find more efficient drug forms and to reduce the toxicity of free DOX. Increasing evidence firmly suggests that the underlying mechanism for anthracycline cytotoxicity is the induction of apoptosis through intracellular-mediated signaling pathways [3,4]. It has also been shown that adriamycin initiates inhibition of the growth-related NADH oxidase in the plasma membrane of cancer cells associated with apoptosis [5]. Nevertheless, the events in DOX-induced apoptosis are poorly understood and determining the mechanisms of DOX membrane effects remains a challenge.

The purpose of this work was to investigate the binding of DOX, immobilized on a magnetic nanomaterial, to intact human erythrocytes, and

*Corresponding author. Institut für Experimentelle Onkologie und Therapieforschung TUM, Ismaninger Str. 22, D-81675 München, Germany. Tel.: +49 16095121846.
E-mail address: Olga.Mykhaylyk@gmx.net (O. Mykhaylyk).

0304-8853/$ - see front matter © 2005 Elsevier B.V. All rights reserved.
doi:10.1016/j.jmmm.2005.02.041

to test the effects of this conjugate on signal transduction in human erythrocytes using quantitative determination of the intracellular cAMP and cGMP pools and the stable nitric oxide (NO) metabolites, NO_2^- and NO_3^-. Human erythrocytes were chosen as a model cell system due to the known interactions of DOX with blood components. These interactions determine, to a great extent, DOX pharmacokinetics [6]. The DOX-erythrocyte binding mechanisms include the embedding of DOX into the lipid matrix, the insertion of DOX into the erythrocyte stroma using the 'flip-flop' mechanism [7], or, depending on the level of cholesterol in the membrane, using a specific transporter [8].

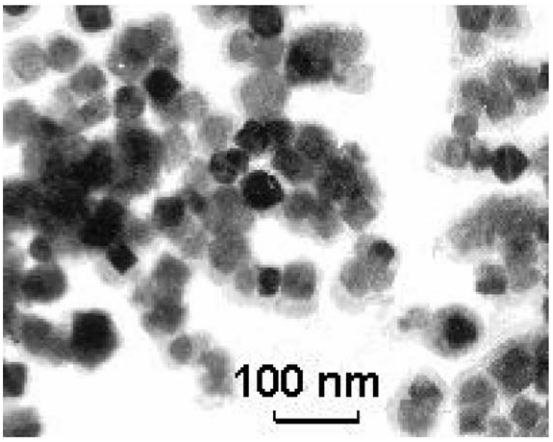

Fig. 1. Electron micrograph of the DOX-M conjugate sample.

2. Experimental

All chemicals were purchased from Sigma-Aldrich. Nanodispersed magnetite was modified by oligomerization of γ-aminopropyltriethoxysilane and activated with 1,6-diisocyanatohexane as described elsewhere [9], followed by chemisorption of hydroxyethylstarch from aqueous solution and repeated activation with 1,6-diisocyanatohexane. The mean diameter of the particle core was 24 ± 19 nm according to electron microscopy data (Fig. 1) and the average nanocrystal size was 30 nm, as calculated from the broadening of the main magnetite peak in the X-ray diffraction pattern. To synthesize a set of doxorubicin magnetic conjugates (DOX-M), DOX was chemisorbed on the surface of the activated nanocarrier from aqueous solution, pH 6.0, followed by chemisorption of O-(2-Aminoethyl)polyethylene glycol 3000 (APEG) from a 2.5% solution in water. The activated carrier with chemisorbed APEG was used as a reference sample. The concentration values of immobilized DOX in DOX-M conjugates were estimated from the decrease in optical density of the contact solutions at $\lambda = 486$ nm, $\varepsilon = 7.50 \times 10^3\,M^{-1}\,cm^{-1}$ and found to be 0.16, 0.4, 1.2, 6.1, and 25.1 mg DOX/g activated carrier, respectively. The cytotoxicity of conjugated DOX in vitro against A2780 human ovarian carcinoma and KB human epidermoid oral cavity cancer cell lines was close to that of free DOX.

Packed erythrocytes from three different donors were washed twice with physiological saline using a commonly accepted method based on differential centrifugation. To study DOX-M conjugate binding, washed erythrocytes (5×10^7 cells/ml of incubation medium) were pre-incubated at 37° for 30 min and aliquots of the DOX solutions in physiologic saline were added to achieve final DOX concentrations in the range of 10^{-12}–10^{-5} M. This erythrocyte solution was incubated at 37° with gentle agitation for 15 min. Thereafter, 0.1 ml portions of the DOX-M suspensions were added to the mixture, resulting in a ratio of *conjugate particles:erythrocytes* of 4×10^3:1. Samples were incubated for 15 min at 37 °C with gentle agitation followed by magnetic separation of the DOX-M conjugate-labeled cells using a permanent magnet. We measured the optical density of the supernatant at 532 nm (D_{532}) to determine concentration of erythrocytes remaining in suspension. The percentage of cells binding magnetic carrier particles was defined by the decrease in cell concentration in the supernatant, after magnetically separating the cells, as $(1 - D_{532}/D^0_{532})$ (%). Each concentration point represents the mean of nine measurements (three independent measurements for erythrocytes from three different donors).

DOX-M nanoparticle ordering in the erythrocyte suspension was investigated by small angle neutron scattering (SANS), which was performed on frozen erythrocyte suspensions at −10 °C using a "Yellow Submarine" spectrometer at the Budapest Neutron Center ($\lambda = 4.08$ and 8.16 Å). A linear chain model was used to fit the data. DOX-M conjugate samples with 6.1 mg immobilized DOX/g carrier were measured using this technique. A DOX-M suspension in physiological saline was added to the washed erythrocyte suspension (hematocrit index = 0.4) at 37 °C, at a final concentration of 3.2×10^3 conjugate particles/cell and frozen immediately (sample a), after a 10 min incubation (sample b), or after a 30 min incubation (sample c). Another erythrocyte sample was preincubated for 10 min with 0.2 μM free DOX to saturate binding sites, then the DOX-M suspension was introduced as above, and frozen after a 30 min incubation (sample d).

To test the effects of the preparations on signal transduction by human erythrocytes, a suspension of 5×10^7 cells/ml was quickly mixed with aliquot of free or conjugated DOX in saline (final concentration from 0 to 8 μg DOX/ml or 9×10^{-8}–1.5×10^{-5} M) and incubated at 37 °C for 15 or 30 s (early interaction period), or 15 or 30 min (late interaction period). Upon incubation, 8×10^4 particles of DOX-M conjugate/cell were applied to ensure saturation of the binding sites. The observed effects on signal transduction were stipulated solely by immobilized DOX, as DOX desorption from the conjugate during the observation times was negligible (less than 0.4% over 1 h, Fig. 2) and the conjugate did not penetrate the cell over the duration of the experiment (Fig. 4).

The concentrations of cGMP and cAMP extracted into ethanol were determined using an Amersham radioimmune analysis test system and a Beckman beta counter [10]. The reference concentrations in the erythrocyte suspension were 0.49 ± 0.17 and 38.3 ± 6.4 pmol/g protein for cGMP and cAMP, respectively. Each data point represents a mean of four measurements (probe duplicates for erythrocytes from two different donors).

To determine the content of stable NO metabolites (NO_2^- and NO_3^-), the cell suspension was

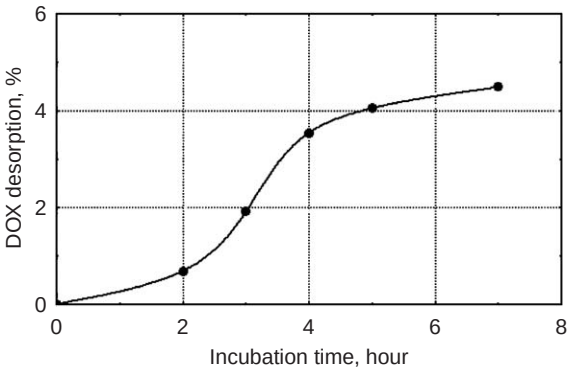

Fig. 2. DOX release profile vs. incubation time for DOX-M conjugate at 37 °C in a physiological solution, pH 7.4.

added to an equal volume of 1 N $HClO_4$ solution, following the incubation period. NO_2^- content in deproteinized aliquots was determined using Griess reactant with Green's method [11]. NO_3^- content was determined using a modified colorimetric method [12] in which the dinitroderivative brucine, 10,11-dimetoxystrichnine, was used in place of strychnine. The brucine reactant was added to deproteinized probes in a *probe:reagent* ratio of 2:1, incubated for 10 min at 100 °C, and the extinction $D_{405\,nm}$ was measured. Data represent the mean of 12 measurements performed in four parallel probes from three different donors for each time point. The reference concentrations in the erythrocyte suspensions were 0.600 ± 0.055 nmol/g protein and 10.3 ± 0.5 μmol/mg protein, for NO_2^- and NO_3^-, respectively.

The protein content was determined by the Bradford Assay using bovine serum albumin as a standard.

Erythrocyte acid resistance was determined using a kinetic method [13]. Changes in extinction were determined at 750 nm every 30 s throughout the hemolysis of intact and $NaNO_2$-damaged erythrocytes in the presence of different concentrations of free and conjugated DOX.

3. Results and discussion

DOX immobilized at the surface of magnetite nanoparticles retained its ability to bind its target

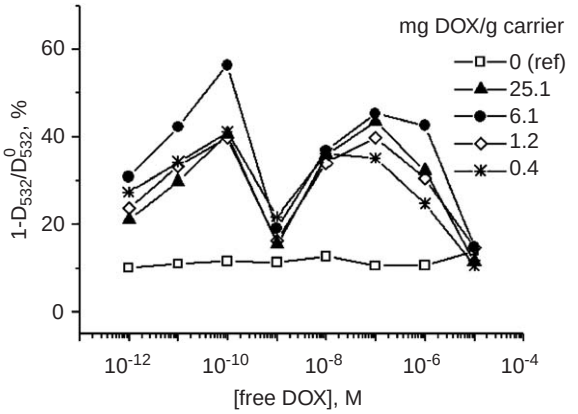

Fig. 3. Mean values of erythrocyte binding for DOX-M conjugates with varying ratios of immobilized DOX to free DOX in the incubation medium.

receptors in competition with free DOX. Fig. 3 shows the binding of immobilized DOX to human erythrocytes in the presence of 10^{-12}–10^{-5} M free DOX. The introduction of free DOX inhibited immobilized DOX binding, providing evidence of specific DOX binding at the cell surface. As shown by the concurrent binding measurements (Fig. 3), there are two highly specific binding sites (receptor pools) for DOX at the plasma membrane of human erythrocytes. No specific binding with the plasma membrane was observed for the nanodispersed magnetite without immobilized DOX; however, a small amount of magnetite bound to the erythrocytes. This nonspecific binding of magnetic nanoparticles resulted in a substantial protector effect against the hemolysis of erythrocytes damaged by $NaNO_2$ treatment (Table 3, [DOX] = 0).

Fig. 4 shows the electron dense particles of the DOX-M conjugate attached to a mouse erythrocyte membrane in the blood capillary lumen of the cerebral cortex, after i.v. injection of the conjugate. The attached particle density is close to 100 particles/μm^2 of erythrocyte surface, which, when accounting for the apparent erythrocyte area ($\approx 90\,\mu m^2$), corresponds to at least 9×10^3 DOX binding sites at the cell surface.

Using the SANS method, aggregates of the DOX-M nanoparticles with an R_g of 90 nm were detected immediately after introduction of the

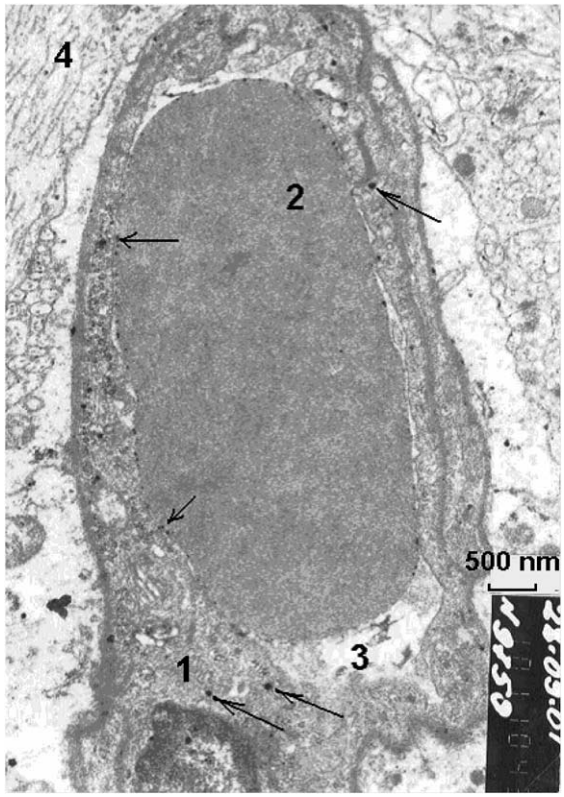

Fig. 4. Mouse cerebral cortex 1 h after i.v. injection of 25 μg DOX-M conjugate (or 0.15 μg DOX)/g (w/w): arrows denote electron dense particles distributed in endothelial cells (1), in the blood capillary lumen (3) and in neurophyl (4), and attached to the membrane of erythrocyte (2).

DOX-M preparation into the erythrocyte suspension (Fig. 5a). Upon incubation, SANS intensity distributions changed (Fig. 5b and c) and the gyration radius of the scattering centers (DOX-M) decreased to 50 and 15 nm after 10 and 30 min of incubation, respectively, from the initial 90 nm as shown in Fig. 5a. The decrease in the scale of the structures is consistent with desaggregation of the material due to interaction with erythrocytes (adsorption at the plasma membrane). Preincubation with free DOX prior to introduction of the nanomaterial resulted in the inhibition of desaggregation: R_g was estimated to be 135 nm after 30 min of incubation (Fig. 5d). This result can be interpreted in terms of inhibition of the specific adsorption of the immobilized DOX-containing nanomaterial by free DOX, confirming the specific

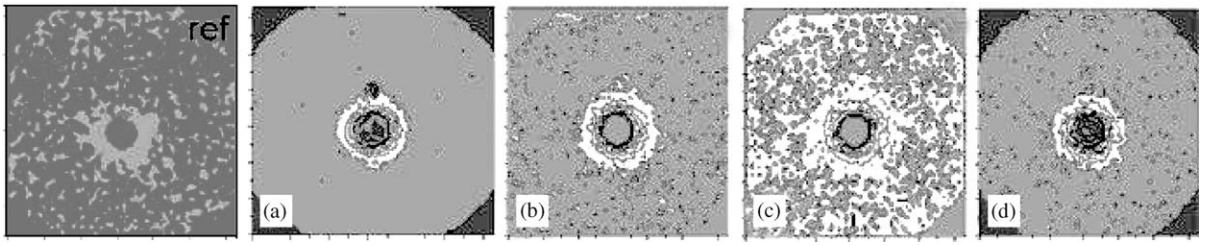

Fig. 5. 2D SANS intensity patterns, corrected for background transmission, for samples of human erythrocytes (ref) and after introduction of 3.2×10^3 DOX-M conjugate particles per cell (6.1 mg DOX per gram carrier). Samples were frozen immediately (a), after 10 min of incubation (b), and after 30 min of incubation (c). The sample in (d) was preincubated for 10 min in the presence of 0.2 μM free DOX, then the DOX-M suspension was introduced, followed by 30 min of incubation and freezing. The vertical and horizontal dimensions of the plots correspond to $2q_{max}$ momentum transfer, and $q_{max} = 0.053\,\text{Å}^{-1}$ (S–D = 5.5 m; $\lambda = 8.13$ A).

binding of the immobilized DOX preparations to the erythrocyte plasma membrane. Another important question is whether DOX binding performs a receptor function and modulates signal transduction in erythrocytes.

The effects of rapid cell activation (within 30 min) due to interaction with free and immobilized DOX were compared in the concentration range of 9×10^{-8}–1.5×10^{-5} M DOX. We observed immediate and similar effects of free and immobilized DOX on the formation of second messengers (Table 1), resulting in an increase in NO metabolites (Fig. 6 to the right), steady state cGMP concentrations, and a reciprocal decrease in cAMP levels (Fig. 6 to the left).

An overall significant increase in the cGMP/cAMP ratio was observed (Table 2). For free and conjugated DOX, maximal [cGMP]/[cAMP] ratios were 33- and 25-fold greater, respectively, than the basal ratios at [DOX] = 0. The NO metabolites were 4.4- and 5.5-fold greater than basal NO metabolites at [DOX] = 0 for NO_2^-, and 5.5- and 5-fold greater for NO_3^-. Similar changes of the tested parameters in response to free and immobilized DOX preparations provided evidence that immobilized DOX retained its ability to modulate cell signal transduction, in a similar manner to free DOX. It is also important that the termination of cell activation occurred after 30 min of incubation.

Preparations with lower immobilized DOX concentrations (0.4 and 2 μg/ml) can be more effective than those with high concentration (8.25 μg/ml) in achieving the highest signaling effect. Interestingly, the highest specific cytotoxicity in both A2780 human ovarian carcinoma and KB human epidermoid oral cavity cancer cell lines occurred for conjugates with a DOX concentration of 6.1 mg/g carrier, which was also one of the most effective in generating immobilized DOX signal effects (Figs. 6).

A substantial increase in NO production as a result of free and immobilized DOX signal action can be indicative of a physiological increase in intracellular Ca^{2+}-ion concentration, with subsequent constitutive NO-synthase activation. Both pathways for $[Ca^{2+}]_i$ increase are associated with activation of the phospholipid signal system. One pathway is characterized by phosphatidyl inositol hydrolysis: an increase in inositol phosphates and diacylglycerol, the second messengers responsible for the mobilization of cytoplasmic free calcium and activation of protein kinase C. It must be noted that the main conjugated calcium store in erythrocytes is in the plasma membrane (calcium is mainly associated with phosphatidyl inositol phosphates and sphingomyelin). Thus, another pathway for $[Ca^{2+}]_i$ increase is sphingomyelin hydrolysis with ceramide production. Ceramide can be further hydrolyzed to sphingosine, accompanied by Ca^{2+} release from the plasma membrane. Sphingosine is known to be an apoptosis trigger [3]. The increase in cGMP levels upon free and immobilized DOX signal action is apparently stipulated by the activation of soluble guanylate cyclase by NO. The reciprocal decrease in cAMP levels in the early period of DOX signal action can be also stipulated by an NO increase, as NO is an inhibitor of the membrane adenylate cyclase [14].

Table 1
Concentrations of the secondary messengers cAMP, cGMP and NO metabolites NO_2^- and NO_3^- in human erythrocytes incubated in the presence of different concentrations of free DOX or immobilized DOX (DOX-M conjugates) for 15 s, 30 s, 15 min and 30 min after their introduction into erythrocyte suspensions

Preparation	[DOX] (μg/ml)	15 s	30 s	15 min	30 min
$[cAMP]/[cAMP]_{[DOX]=0}$ (M, $n=4$)					
Free DOX	0.05	0.90	0.92	0.43**	0.71
	0.10	0.80	1.24	0.46**	0.72
	0.40	0.73	0.93	0.50**	0.65
	2.00	0.64	1.12	0.62*	1.13
	8.00	0.96	0.72	0.78	1.23
DOX-M conjugates	0.05	1.01	1.04	0.77	0.77*
	0.10	0.78	0.81	0.66	0.72*
	0.40	0.91	0.67	0.49*	0.63*
	2.00	0.56	0.69	0.68	0.80
	8.00	0.69**	0.93	0.71	0.70
$[cGMP]/[cGMP]_{[DOX]=0}$ (M, $n=4$)					
Free DOX	0.05	1.3	2.3	8.6**	8.5**
	0.10	3.3**	2.5**	11.9**	12.2**
	0.40	4.4**	3.0*	17.5*	21.6*
	2.00	3.1**	2.3**	14.3*	11.9*
	8.00	2.6*	2.5	12.4*	11.8*
DOX-M conjugates	0.05	2.87**	1.63	6.52**	5.11**
	0.10	3.62**	1.77	6.76*	7.37**
	0.40	5.02*	1.80	11.54**	9.93*
	2.00	2.40	3.29	11.47**	9.48**
	8.00	1.3	2.3	8.6**	8.5**
$[NO_2^-]/[NO_2^-]_{[DOX]=0}$ (M, $n=12$)					
Free DOX	0.05	0.8	1.7**	1.9**	0.8
	0.10	0.9	2.1**	2.2**	1.1
	0.40	1.2	2.0**	2.0**	1.2
	2.00	1.8*	3.6**	2.9**	1.3
	8.00	1.9**	4.4**	2.8**	0.9
DOX-M conjugates	0.05	1.5*	2.1**	1.4	1.8**
	0.10	1.0	2.3**	1.9**	2.0*
	0.40	1.9**	2.5**	1.6*	2.0
	2.00	2.2**	3.8**	1.8*	3.1**
	8.00	3.9**	5.5**	2.2*	1.8
$[NO_3^-]/[NO_3^-]_{[DOX]=0}$ (M, $n=12$)					
Free DOX	0.05	2.03**	2.54**	2.35**	2.21**
	0.10	2.72**	2.53**	3.11**	2.84**
	0.40	2.88**	3.79**	2.95**	3.75**
	2.00	3.63**	4.75**	2.79**	2.06**
	8.00	4.04**	5.16**	3.59**	2.23**
DOX-M conjugates	0.05	1.71**	3.08**	1.59**	1.87**
	0.10	2.37**	3.68**	1.90**	2.36**
	0.40	3.61**	4.23**	1.76**	1.76**
	2.00	4.52**	4.64**	1.64**	2.16**
	8.00	4.57**	5.02**	1.61*	2.27*

*$p<0.05$, **$p<0.01$, mean differs significantly from reference data at [DOX] = 0.
Data were normalized to the values determined at [DOX] = 0 without the addition of DOX (for free DOX) or in the presence of the carrier itself (for DOX-M conjugate).

In the investigated concentration range (0.05–8.25 μg/ml) free DOX had no hemolytic effect on intact erythrocyte membranes, and, in fact, stabilized the plasma membrane and increased the acid resistance of intact erythrocytes and $NaNO_2$-damaged erythrocytes (Fig. 7, Table 3). Sodium nitrite provokes oxidative damage of the erythrocyte plasma membrane and stroma hemoglobin, resulting in substantial membrane labilization and decreased erythrocyte acid resistance, as evidenced by the t_{max} shift to the left compared to the values for intact washed erythrocytes. Introduction of free or conjugated DOX into the lysis medium caused a substantial dose-dependent increase in the acid resistance of damaged erythrocytes, as confirmed by the kinetic data on erythrocyte acidic hemolysis (Table 3). The increase in the erythrocyte stability index, the time for onset of hemolysis, the time to hemolysis termination and total duration of hemolysis, the increase in the number of fractions in the erythrogram, and the shifting of the kinetic curve maximum to the right, all imply that an increase in erythrocyte stability has occurred in the presence of free or conjugated DOX.

An important question is: to what extent are the signal effects of free and immobilized DOX responsible for the DOX cytotoxic activity observed in vitro and in vivo? Highly active isoforms of iNOS are present in many cell types. For DOX, both activation of iNOS enzyme activity (and even the corresponding activation of gene expression) and its inhibition have been previously reported [15,16].

The role of NO in cancerogenesis is not yet been determined. Although NO has been established as a potent inducer of apoptosis in different cell types, contradictory effects have been reported [17]. It was shown that low NO concentrations can contribute to cell survival, whereas higher NO concentrations are pathological and promote cell destruction [18,19]. The final result (activation or inhibition of apoptosis) may be determined by NO concentrations and the presence of other pro-apoptotic and anti-apoptotic factors. A significant increase in the cGMP level is considered to be an apoptotic signal. Down-regulation of cAMP also results in a shift toward apoptosis.

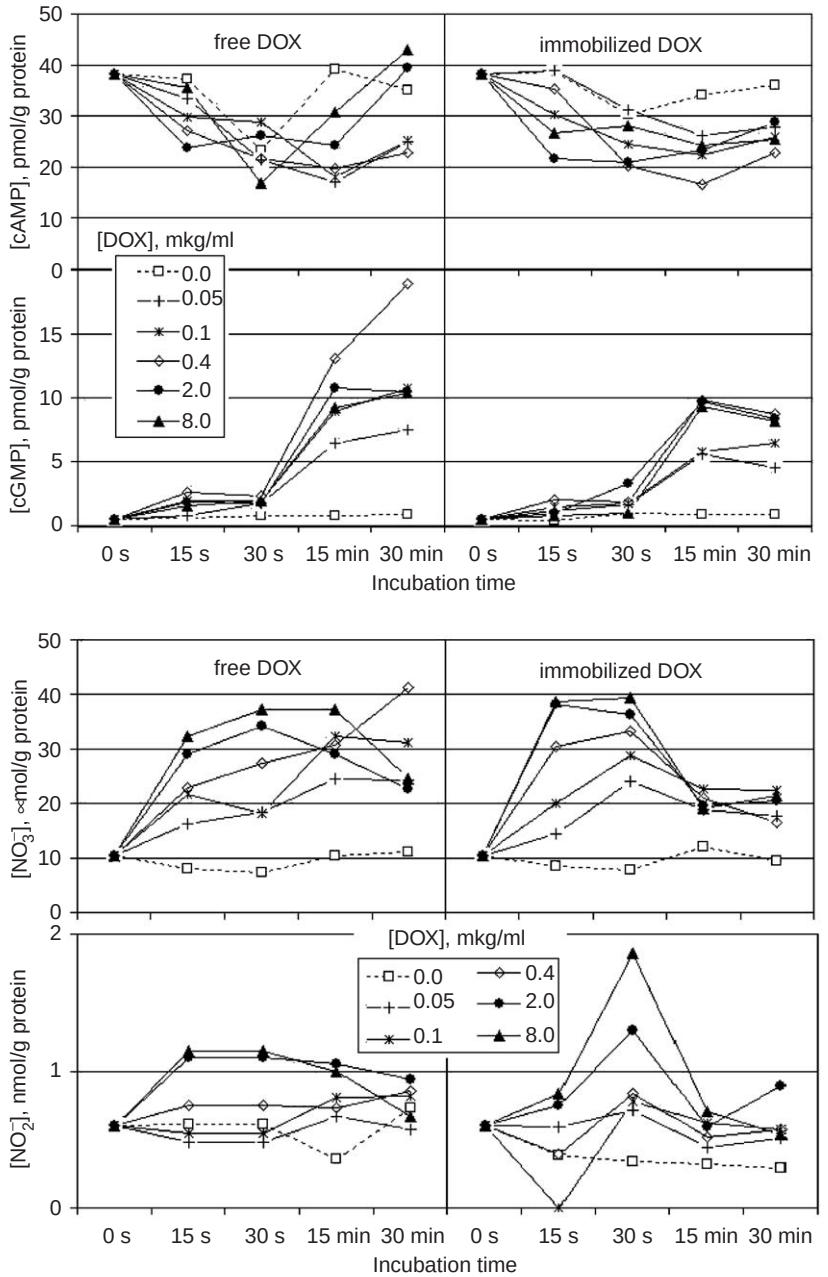

Fig. 6. Concentrations of the cyclic purine nucleotides cAMP and cGMP, and the NO metabolites, NO_3^- and NO_2^-, in human erythrocytes incubated in the presence of different concentrations of free DOX or immobilized DOX (DOX-M conjugates) for 15 s, 30 s, 15 min and 30 min.

In particular, BAD is a pro-apoptotic Bax-like protein that is reversibly modulated by cAMP-mediated phosphorylation, i.e., phosphorylated BAD is unable to promote apoptosis [20]. The inhibition of NADH oxidase related to the down-regulation of cAMP in cancer cells is also

associated with growth inhibition and activation of apoptosis [5].

4. Conclusion

There are specific binding sites for DOX at the plasma membrane of human erythrocytes. The DOX-M conjugate does not penetrate into the cell for at least an hour. It has been established that free and conjugated DOX are antagonists of the erythrocyte receptors coupled to the phospholipid signal system. This is evidenced by an increase in NO and cGMP levels. On the basis of the experimental data obtained, one can concede the following sequence of events initiated by DOX interaction with erythrocyte's surface: DOX → binding to receptor(s) in the plasma membrane conjugated with phospholipase C → activation of phosphoinositol hydrolysis → generation of inositoltriphosphate and diacylglycerol → increase in cytosolic calcium concentrations ($[Ca^{2+}]_i$) → activation of Ca-dependent (constitutive) NO-synthase → NO generation → activation of the cytosolic (soluble) guanylate cyclase → cGMP generation. The decrease in cAMP levels as a consequence of DOX signaling may be caused by an increase in NO production (adenylate cyclase inhibition), or by increased cGMP levels resulting in the activation of cAMP-phosphodiesterase, which hydrolyzes cAMP with AMP production. The powerful membrane-stabilizing action of low free and conjugated DOX concentrations may signify the underlying importance of membrane events in the specific anticancer action of this anthracycline antibiotic. The relative role of cell signaling in DOX anticancer activity and its clinical significance is still unclear; nevertheless the features described here can suggest methods for the optimization of DOX formulations.

Table 2
[cAMP]/[cGMP] ratio ($M, n = 4$) in human erythrocytes incubated in the presence of different concentrations of free DOX or immobilized DOX (DOX-M conjugates) for 15 s, 30 s, 15 min and 30 min after their introduction into erythrocyte suspensions

Preparation	[DOX] (μg/ml)	15 s	30 s	15 min	30 min
		$\frac{[cGMP]/[cAMP]}{([cGMP]/[cAMP])_{[DOX]=0}}$			
Free DOX	0.05	1.4	2.1	20.0*	11.1**
	0.10	4.2**	2.2	33.3*	16.7**
	0.40	5.9**	2.4	33.3*	25.0**
	2.00	3.8**	2.2	20.0*	7.1**
	8.00	2.8**	0.5	16.7*	7.1**
DOX-M conjugates	0.05	3.2*	1.0	9.1*	6.7
	0.10	5.0**	1.2	11.1*	11.1**
	0.40	6.3**	2.7*	25.0*	12.5**
	2.00	2.0	3.7**	20.0*	12.5**
	8.00	3.8*	0.8	14.3*	14.3**

*$p < 0.05$, **$p < 0.01$, mean differs significantly from reference (ref) data at [DOX] = 0.
Data were normalized to the values determined at [DOX] = 0 without the addition of DOX (for free DOX) or in the presence of the carrier itself (for DOX-M conjugate).

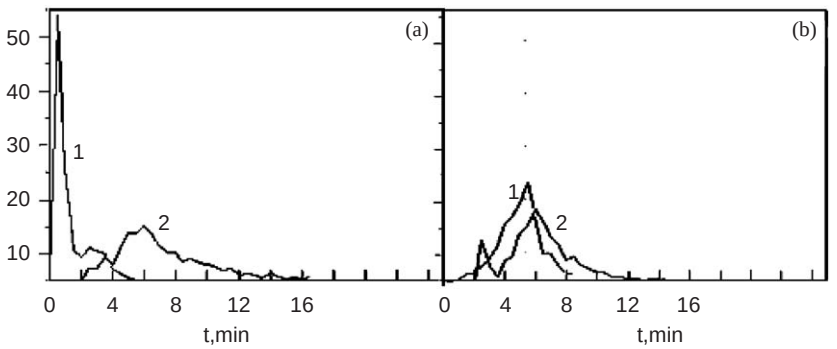

Fig. 7. Acid erythrograms of $NaNO_2$-damaged human erythrocytes. Panel (a) shows the reference curve (1) and the curve generated in the presence of 8 μg free DOX/ml (2). Panel (b) shows the curve in presence of the carrier, [DOX] = 0 (1), and the curve generated in the presence of 8 μg immobilized DOX/ml (2). Abbreviations: *t*, time.

Table 3
Kinetic parameters of acid hemolysis of human erythrocytes damaged with $NaNO_2$ performed in the presence of different free and immobilized DOX concentrations

[DOX] (μg/ml)	Stability index	t_s (min)	t_t (min)	$\Delta t = t_t - t_s$ (min)	n (units)	t_{max} (min)
Free DOX						
0	128	0	6	6	2	0.5
0.05	455	2	10.5	8.5	3	3
0.1	552	2	11	9	4	5
0.4	675	1.5	16	14.5	8	5
2.0	699	2.5	19.5	17	7	4.5
8.0	717	2.5	17	14.5	11	6
DOX-M conjugate						
0	505	1.5	9	7.5	4	5.5
0.05	548	0.5	12.5	12	4	5.5
0.1	602	1.5	13	11.5	5	6
0.4	614	1	20.5	19.5	8	5.6
2.0	699	1	23.5	22.5	11	5.6
8.0	626	2.5	15	11.5	7	6

Abbreviations: starting time of hemolysis, t_s: time of hemolysis termination, t_t: total duration of hemolysis, ($\Delta t = t_t - t_s$): number of erythrocyte fractions, n: position of the kinetic curve maximum, t_{max}.

Acknowledgments

We thank Dr. L. Stechenko for performing the electron microscopic studies. We also thank Dr. G. Solyanik for testing the anticancer activity of DOX conjugates in vitro and Dr. J. Gerloff for valuable discussions.

References

[1] T.R. Triton, G. Yee, Science 217 (1982) 248.
[2] P. Vichi, T.R. Triton, Cancer Res. 52 (1992) 4135.
[3] O. Cuvilier, V.E. Nava, S.K. Murtthy, Cell Death Differ. 8 (2001) 162.
[4] S. Di Bartolomeo, F. Di Sano, M. Piacentini, et al., J. Neurochem. 75 (2000) 532.
[5] D.J. Morre, C. Kim, M. Paulik, et al., J. Bioenerg. Biomembr. 29 (1997) 269.
[6] D. Schrijvers, M. Highlez, E. Bruzn, et al., Anti-Cancer Drugs 10 (1999) 147.
[7] R. Regev, G.D. Eytan, Biochem. Pharmacol. 54 (1997) 1151.
[8] S. Awasthi, S.S. Singhal, S. Pikula, et al., Biochemistry 37 (1998) 5239.
[9] O. Mykhaylyk, A. Kotzuruba, O. Buchanevich, et al., J. Magn. Magn. Mater. 225 (2001) 226.
[10] J.J. Keirus, M.A. Wheeler, M.W. Bitensky, Anal. Biochem. 61 (1974) 336.
[11] L.C. Green, A.W. David, J. Glogowski, et al., Anal. Biochem. 126 (1982) 131.
[12] N.R. Bank, H.S. Aynedjian, Kidney Int. 43 (1993) 1306.
[13] I.A. Terskov, I.I. Gittelson, Biophysics 2 (1957) 259 (in Russian).
[14] S. Wang, L. Yan, R.A. Weslez, et al., J. Biol. Chem. 272 (1997) 5959.
[15] R. Inagaki, T. Taniguchi, T. Sakai, Gen. Pharmacol. 32 (1999) 185.
[16] T. Sakai, I. Muramatsu, N. Hazashi, et al., Gen. Pharmacol. 27 (1996) 1367.
[17] J.S. Beckman, W.H. Koppenol, Am. J. Physiol. 271 (1996) C1424.
[18] Y.H. Shen, X.L. Wang, D.E.L. Wilcken, FEBS Lett. 433 (1998) 125.
[19] J. Haendeler, U. Weiland, A.M. Zeiher, et al., Biol. Chem. 1 (1997) 282.
[20] J. Zha, H. Harada, E. Yang, et al., Cell 87 (1996) 619.